



## SYNTHESIS OF PLANT-MEDIATED SILVER NANOPARTICLES USING *LYCOPERSICON ESCULENTUM* L. EXTRACT AND EVALUATION OF THEIR ANTIMICROBIAL ACTIVITIES

<sup>1</sup>SMARANIKA DAS, <sup>2</sup>UMESH KUMAR PARIDA AND <sup>2</sup>BIRENDRA KUMAR BINDHANI\*

<sup>1</sup>Department of Botany, Ravenshaw Junior College, Cuttack, Odisha, India

<sup>2</sup>School of Biotechnology, KIIT University, Bhubaneswar, Odisha, India

### ABSTRACT

Present investigation deals with the synthesis of silver nanoparticles (AgNPs) from *Lycopersicon esculentum* L. through simple and eco-friendly chemical methods. In this technique, silver nitrate has been used as the metal precursor and hydrazine hydrate as a reducing agent. The nanoparticles thus obtained from *Lycopersicon esculentum* L. have been analysed and characterised by Scanning Electron Microscopy (SEM) and Energy-Dispersive Spectroscopy (EDX). The average diameter of the AgNPs, whose morphology has been determined by SEM, was found to be 70 - 90nm. The EDX analysis was carried out with a range of 2–4 keV which confirmed that the nanoparticles dispersion in the presence of elemental silver with no other detectable impurity peaks. The silver nanoparticles were characterized which have bright prospects for application in different medical and industrial fields. The results showed that the silver nanoparticles, which are susceptible to different for each and every microorganism. The antimicrobial activity of silver nanoparticles (AgNPs) has been evaluated with *Escherichia coli*, gram negative bacteria. Importantly, though the kinetics of killing were altered, AgNPs retained potent bactericidal activity against *E. coli* at low pH. A molar-to-molar comparison was carried out to know the efficacy of AgNPs as compared to metronidazole (MTZ), amoxicillin (AMX) and clarithromycin (CLR).

**KEYWORDS:** Silver Nanoparticles (AgNPs), *Lycopersicon esculentum* L., Biosynthesis, Antimicrobial Activity, *Escherichia coli*.



**BIRENDRA KUMAR BINDHANI**

School of Biotechnology, KIIT University, Bhubaneswar, Odisha, India

## INTRODUCTION

The past few years have been witness to the growing need to develop non-toxic chemicals, environmentally benign solvents and renewable materials [1-8]. There are several classes of nanoparticles, available amongst which metal nanoparticles specially silver and gold nanoparticles are most sought after due to their application in various fields of science and technology [7]. Now a day various methods are available for the synthesis of silver and gold nanoparticles, for example, reduction of the solution; thermal synthesis [9]; electrochemical synthesis [10]; microwave-assisted synthesis [11]; and most recently, usage of green chemistry [12, 13]. Using plants in the biosynthesis of metal nanoparticles, is being sought after as a suitable alternative over chemical procedures and physical methods. Bioreduction of metal nanoparticles using a combination of biomolecules found in plant extract, such as enzymes, proteins, amino acids, vitamins, polysaccharides, and organic acids like citrates is convenient as well as environmentally safe. Extracts from plants may act as both reducing and sealing agents in nanoparticle synthesis [14]. Biosynthesis of silver nanoparticles in plants such as *Memecylon umbellatum* [15], *Ocimum sanctum* [16], *Dillenia indica* [17], *Trachyspermum ammi* and *Papaver somniferum* [18], *Macrotyloma uniflorum* [19], *Putranjiva* [20] have been reported by several researchers. However, in the present-day scenario, the potential of more and more plants as green biosynthesis of nanoparticles is yet to be fully explored. The present experimental material, fresh tomato juice contains major polysaccharides such as

pectins, arabinogalactans, xylans, arabinoxylans, and cellulose. Among the amino acids Glutamic acid only makes 45% of the total weight of free amino acids in fresh tomato juice with aspartic acid being the next highest in concentration. Citric acid is the most abundant organic acid present in the tomato juice, with little amount of malic acid [21, 22]. Hence the water extract of the tomato juice mostly contains proteins, polysaccharides, organic acids amino acids, and vitamins. May be the gold and silver ions are reduced by citric acid and aspartic acids present in the aqueous extract while the soluble proteins and other amino acids help in the stabilization of metal nanoparticles. As reported by various researchers that silver nanoparticles AgNPs are very effective against a broad range of microorganisms [23-25]. It has been discovered recently that many organelles when surrounded by silver ions reduce  $Ag^{+3}$  to  $Ag^0$ . Thus, green biosynthesis of AgNPs using organelles are an exciting and interesting alternative method which may currently be used for the experiment. Hence, with alacrity the authors of the present paper try to investigate the possibility of biosynthesizing AgNPs using *Lycopersicon esculentum* as biological templates. Ample amount of *Lycopersicon esculentum* L. are available in odisha. The present investigation deals with the synthesis of silver nanoparticles and characterization using *Lycopersicon esculentum* (Figure 1). Further, the antimicrobial action of silver nanoparticles (AgNPs) was studied against pathogenic gram positive bacteria.

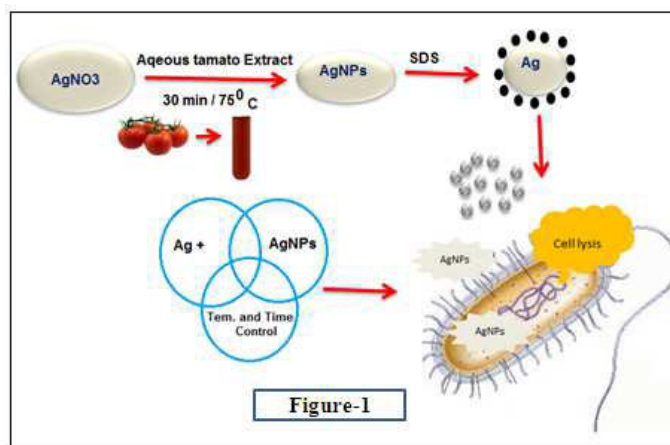


Figure 1

**Schematically representations of synthesis of silver-based nanoparticles inhibit the Bacterial cell.**

## MATERIALS AND METHODS

All the chemicals like Silver nitrate (99.9%), absolute alcohol (99.9%), hydrazine hydrate, sodium citrate, sodium dodecyl sulfate (SDS) has been purchased from Nobel Enterprises, India. All solutions were prepared by using double distilled deionised water for this study.

### Plant Material

OUAT (Orissa University of Agriculture and Technology), Odisha, India has authenticated locally collected plant material *Lycopersicon esculentum* L.

### *Lycopersicon esculentum* Extract Preparation

*Lycopersicon esculentum* L. (Red Tomato) was collected from the market and washed with tap water followed by double distilled water. After removing the skin from the tomato, the whole mass was squeezed and filtered using a whatman filter paper (Maidstone, UK). Then the juice was diluted twice of its volume with double distilled which was used as the tomato extract as solution. Different compositions like 5:5, 6:4, 7:3, 8:2, and 10:0 were prepared by using tomato extract with double distilled for this experiment.

### Synthesis of Silver Nanoparticles

Silver nanoparticles (AgNPs) were formed by the reduction of silver nitrate by using tomato extract (Figure 2). Then, 5ml of a 1mM

aqueous silver nitrate was added drop wise with 5ml of the extract which was cooled in ice-cold water by continuous stirring. Further, cooled the mixture for 10 minutes and then heated at 80°C for 30 minutes. The solution colour was gradually changed starting yellow to deep reddish violet. It indicated that the formation of silver nanoparticles.

### SDS capped SNP in alkaline medium

SNP biosynthesis with SDS has been used as a colorimetric sensor to determine and estimation of the pesticide present in both water and alkaline medium. To control a wide range of insect pests worldwide, pesticide methyl parathion has been used extensively though it is a highly neuro-toxic agricultural chemical. This chemical (i.e., pesticide methyl parathion) residue causes pollution in soil and hazardous effects on human health also. The sensor properties were examined by using UV-visible spectral and changes were also observed because of the addition of methyl parathion at parts per million (ppm) levels [26].

### In vitro stability studies of *Lycopersicon esculentum* L. – AgNPs

Silver nanoparticles mediated test were carried out in the presence of the solutions like NaCl, cysteine, histidine, HSA and BSA to determine the *in vitro* stabilities of *Lycopersicon esculentum* L. In general, 1 ml of Ag nanoparticle solution was added into glass vials containing 0.5 ml of each 5 %

NaCl, 0.5 % cysteine, 0.2 M histidine, 0.5 % HSA, 0.5 % BSA solutions respectively and incubated for 30 min. Then, both identity and stability of AgNPs were calculated after 30 minutes by recording UV absorbance (Figure 3). The retention of nanoparticles was confirmed in all the above mixtures through the plasmon resonance band at ~435 nm. Further, the retention of these nanoparticles compositions was confirmed by TEM measurement and also signifying the Ag nanoconstructs in each medium as robust nature under *in vitro* conditions.

## MEASUREMENTS

### UV-Vis Spectroscopy

UV-visible spectroscopy (UV-1601 pc shimadzu spectrophotometer) or ultraviolet-Visible spectrophotometer (UV-Vis) refers to absorption spectroscopy in the UV-Visible spectral region. It uses light in the visible and adjacent near-UV and near-infrared (NIR)) ranges. The absorption in the visible range directly affects the perceived color of the chemicals involved. In this region of the electromagnetic spectrum, the molecules undergo electronic transitions.

### X-Ray Diffraction (XRD) Measurements

XRD was used to study the phase formation of bioreduced silver nanoparticles. The diffraction data of thoroughly dried thin films of nanoparticles on glass slides was recorded on D 8 Advanced Bruker X-ray diffract meter with Cu K $\alpha$  (1.54 Å) source.

### Fourier Transmission Infra Red Spectroscopy (FTIR)

The FTIR spectrum of *Lycopersicon esculentum* L. extract, AgNO<sub>3</sub> nanoparticle and amine functionalized Ag nanoparticle were recorded using a BIORAD-FTS-7PC type FTIR spectrophotometer.

### Scanning Electron Microscope (SEM) Analysis

SEM analysis was carried out by using Hitachi S - 4500 SEM machine. Thin films of the sample were prepared on a carbon coated copper grid by just dropping a very small amount of the sample on the grid, extra solution was removed using a blotting paper and then the film on the SEM grid were

allowed to dry by putting it under a mercury lamp for 5 min.

### Transmission Electron Microscope (TEM) Analysis

Transmission electron microscope (Philips CM-10) is a microscopy technique whereby a beam of electrons is transmitted through an ultra-thin specimen, interacting with the specimen as it passes through. An image formed from the interaction of the electrons transmitted through the specimen; the image was magnified and focused onto an imaging device.

### Dynamic Light Scattering (DLS)

This is one of the most popular techniques which were used to determine the size of particles. Shining a monochromatic light beam, such as a laser, onto a solution with spherical particles in Brownian motion causes a Doppler Shift when the light hits the moving particle, changing the wavelength of the incoming light. This change was related to the size of the particle. From DLS (Zetasizer, Malvern) it was possible to compute the sphere size distribution and give a description of the particle's motion in the medium, measuring the diffusion coefficient of the particle and using the auto correlation function.

## TEST OF MICROORGANISMS

### Antibacterial Activity

A bacterial strain studied was *Escherichia coli* (ATCC 25922), maintained at 4°C and it was obtained from Department of Botany, Berhampur University, Odisha, India.

### Antimicrobial Assays

Test of antimicrobial activity was tested with synthesized AgNPs by agar disc-diffusion method against pathogenic bacteria (i.e., *Escherichia coli*). Mueller Hinton and Potato Dextrose Agar (PDA) were used for sub-culture of pure cultures of bacterial pathogens. The microbial test organisms were grown in nutrient broth at 37°C for 24 hours. A 500 $\mu$ L aliquot of each organism (1 $\times$ 10<sup>6</sup> cfu/ml) was spread on agar using a cotton swab and allowed to dry for 10 minutes. Paper discs loaded with 50  $\mu$ g/ml AgNPs and reference drugs were placed on

the surface of each cultured plate and incubated at 37°C for 24 hours after which inhibition zones were measured [12]. Experiments were conducted in duplicate and mean results recorded.

### **Determination of killing kinetics of *Escherichia coli***

Silver nanoparticles with particular time required to kill *Escherichia coli* for determination of time kill curves through exposing the different strains to a range of *Escherichia coli* concentrations (10-200 µM) for up to 24 h and which was monitored by CFUs. Near about 1ml of bacterial cultures in liquid form were diluted with of OD 600 of 0.05 in CBBM and which was exposed to AgNPs. About 10 fold serial dilutions of the samples were placed on HBA plates after 0, 1, 2, 4, 6, 8, 10, 20, 22 and 24 h of culture in the presence of AgNPs. Then, it was incubated for 5 – 6 days at 37°C by which CFU point was expressed and enumerated as CFU/ml. The similar volume of *Escherichia coli* cells with PBS (0 µM AgNPs) were considered as a control.

### **Comparative efficacy of AgNPs, AMX, MTZ and CLR against *Escherichia coli***

The antibacterial activity of AgNPs against *Escherichia coli* was compared to that of amoxicillin (AMX), metronidazole (MTZ) and clarithromycin (CLR) using time-kill assays as described above. For these assays, the *Escherichia coli* were exposed to 70 µM or 140 µM SQ109, AMX, MTZ and CLR in 1 ml CBBM. Samples were withdrawn at 0, 0.5, 2, 4, 6, 8, 10, 14, 20, 22, and 24 hours and the number of viable CFU determined as described above.

## **RESULTS AND DISCUSSION**

### **UV-vis spectroscopy**

Biosynthesis of AgNPs by *Lycopersicon esculentum* L. is described by colour change to black due to reduction of Ag<sup>3+</sup> to AgNPs. UV-vis spectroscopy authenticates its formation. The peak at 440 nm establishes the synthesis of AgNPs which is in accordance with the previous reports [27]. The effect of extracts quantity indicates that only 5 ml of the extract was enough to carry

out the reaction at a concentration of 1mM of silver nitrate. As shown in Figure 2A, the SPR band intensity decreases as the volume of extract increases to 5, 10 and 15 ml (containing 0.272 mg/ml total phenols expressed as ascorbic acid equivalent). The higher intensity was obtained at 5 ml which indicates that 5 ml was enough for the reaction. The SPR band intensity decreases due to dilution as the volume of extract increases, similar results were obtained [27, 28]. Figure 2B shows the UV-Vis spectra of the AgNO<sub>3</sub> solution after the addition of 1 ml extract as a function of time. The spectra comprise a fast increasing absorption peak at about 435 nm within the first 20 min (Figure 2) followed by a very slow increase in absorption. An additional absorption band at 460 nm was developed after 30 min from the beginning of the reaction. The peak at 440 nm is characteristic for the transverse plasmon resonance of AgNPs, whereas the peak at 440 nm is characteristic for the longitudinal plasmon resonance of either Ag nanorods or triangular or hexagonal shaped AgNPs. It can be concluded that the reduction of Ag<sup>3+</sup> using *Lycopersicon esculentum* L. extract occurs within 30 min [29]. Though the tomato extract is one of strong reducing agent, but it is not a good capping agent. So, it induces nucleation rapidly, but the growth of silver nanoparticles fails to restrict. Hence, silver nanoparticles were observed polydispersion. The band shifts to 440 nm was observed with the use of 100% tomato extract and significantly decrease the extinction coefficient. This may be due to colloidal instability. The polydispersity and the colloidal instability (agglomeration tendency of silver nanoparticle) may be the reason for a broad spectrum of silver sol along with a shift in the peak position. The shifting of the peak position may be related to the increase of the size of silver nanoparticles [26]. The sensor properties of the SNP were examined in the alkaline solution by the addition of altered amounts of NaOH (0.15 (M)). The pH of the solution was maintained for 9 to 9.5 with NaOH for these studies and stabilised the medium with surfactant SDS. Here, SDS acts as a capping agent, due to which the SPR band shifts to 437nm (Figure 2C). In this case

a comparative sharp spectrum with absorbance at 437 nm was observed. This can be explained by the fact that SDS, being a strong capping agent, stabilizes the silver

nanoparticles as soon as nucleation happens and so restricts the maximum size of the nanoparticles [26].

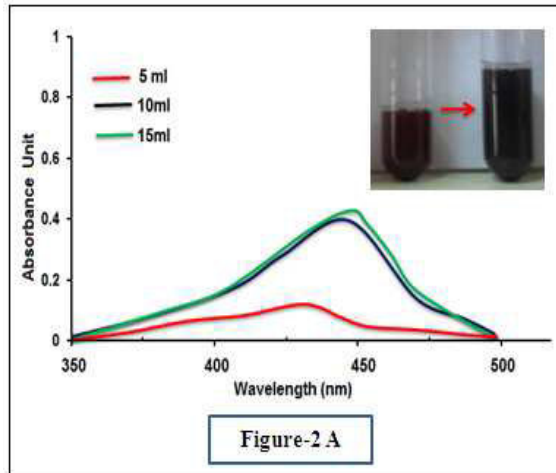


**Figure 2 (A)**

**UV-Visible spectra of Effect of extract concentration on the formation of silver nanoparticles. Inset photos of the particle solutions as a function of concentration of *Lycopersicon esculentum* extract.**

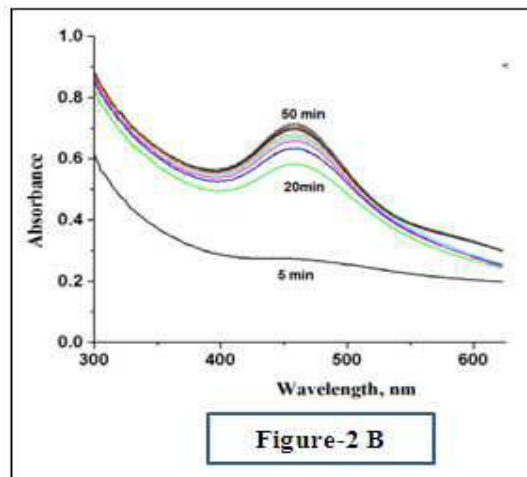


**Figure 2 (B)**

**Kinetics of the formation of AgNPs.  $AgNO_3 = 1mM$ , 1 ml extract in 10 ml flask**

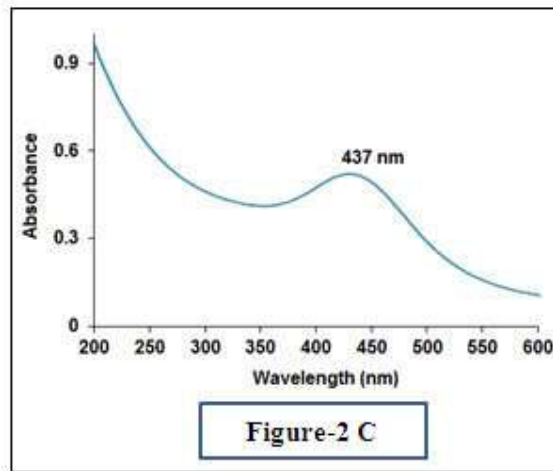


Figure 2 (C)

**UV-visible spectra of *Lycopersicon esculentum* -AgNPs showing in vitro stability of the nanoparticles in SDS medium.**

### **XRD analysis**

The formation of phase synthesized AgNPs was analyzed by X-ray diffraction, which confirmed the bio-reduction of metal nanoparticles is of elemental silver (Figure 3). Existence of peaks (111), (200), (220) and (311) matched with the standard Joint Committee for Powder Diffraction Set (JCPDS) data- 04784 [28]. This confirmed face centered cubic structured AgNPs formation. Peak broadening indicated restricted particle size. Enlarged pattern of

(111) peak is shown in the inset of XRD plot. The crystallitesize was calculated using Scherrer's formula

$$d = \frac{0.9\lambda}{\beta \cos \theta}$$

Here 0.9 is the shape factor, generally taken for a cubic system,  $\lambda$  is the x-ray wavelength, typically 1.54 Å,  $\beta$  is the full width at half the maximum intensity (FWHM) in radians, and  $\theta$  is the Bragg angle. Using the above formula the crystallitesize calculated is ~10 nm [27].

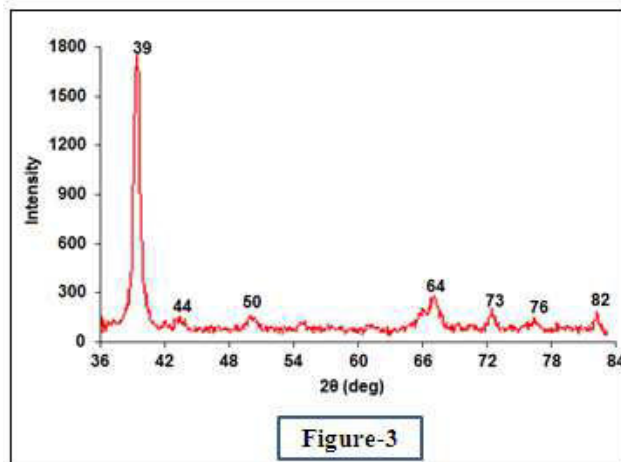


Figure 3

**Representative XRD profile of thin film AgNPs.**



**FTIR**

FTIR results reveal absorption bands at 3432, 3006, 1712, 1525, 1188, 624  $\text{cm}^{-1}$  (*Lycopersicon esculentum* L. extraction) in Figure 4(a); [30] 2998, 1701, 1503, 1174, 612  $\text{cm}^{-1}$  (AgNPs at 80°C) in Figure 4(b); The vibrational bands correspond to the bonds such as aminuteso (N–H), –C=C (alkene),

and C–Cl (Halogens) which were in the region range of 673–3446  $\text{cm}^{-1}$ . The most wide spectrum absorption was observed at 3432 and 1188  $\text{cm}^{-1}$  and it can be attributed to the stretching vibrations of aminuteso (N–H); absorption peaks centered at 1700 and 1500  $\text{cm}^{-1}$  can be attributed to the stretching vibration of –C=C (alkene) [28].

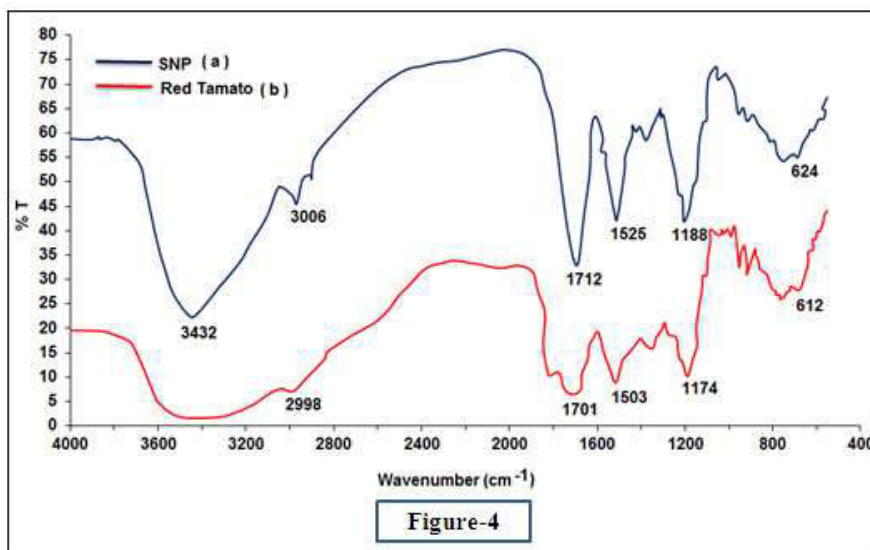


**Figure 4**

**FTIR absorption spectra of *Lycopersicon esculentum* –AgNPs (a), after complete bio-reduction at 50°C (b) *Lycopersicon esculentum* extract.**

**Characterisation of silver nanoparticles by EDX**

Synthesis of AgNPs was measured by EDX spectrum at 25°C and 80°C (Figure 5). The nanoparticles of silver atoms showed very strong signals along with other signals from Si, K, C, and Pt atoms were also recorded. Out of different signals, the C and K signals

were probably due to X-ray emission from proteins/enzymes/carbohydrates present in the *Lycopersicon esculentum* L. extract. Generally, metallic AgNPs showed distinctive absorption peak approximately at 2-4KeV due to SPR [31]. The graph obtained from EDX analysis due the presence of elemental silver, which also supports the XRD results.

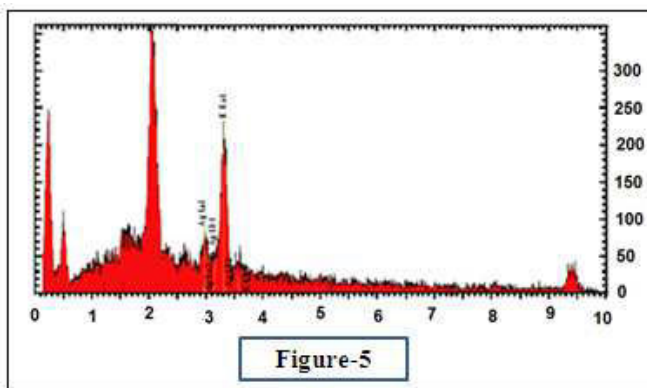


**Figure 5**

**EDX spectrum of AgNPs (a) at 80°C.**



**SEM**

Figure 6 shows representative SEM images recorded at different magnifications from drop-coated films of the Ag nanoparticles synthesised by treating AgNO<sub>3</sub> solution with the extract obtained from *Lycopersicon esculentum* L. The AgNPs were resulted uniform size and predominantly square. These square nanoparticles showed the

average diameter of around 70 – 90 nm in higher magnification. The exact shape of the nanoparticles obtained through biosynthesis with AgNPs from 20ml of leaf extract was not predicted clearly by SEM. A small percentage of resulting nanoparticles were spherical and in the size range 10 – 45 nm. SEM images of nanotriangles in the same suspension are depicted [27, 28, 32].

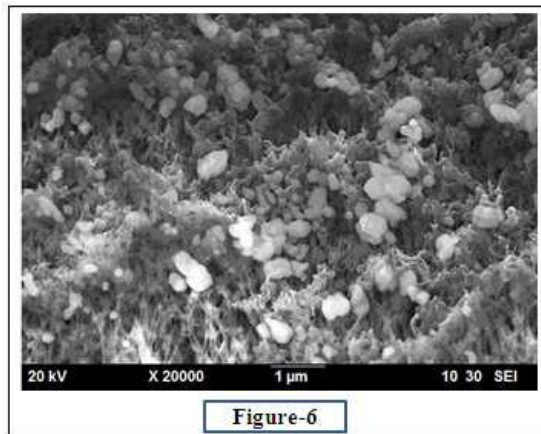


**Figure 6**  
**SEM images of the biosynthesized of AgNPs showing at different magnifications: AgNPs**

**TEM**

The bio-reduced AgNPs were elucidated with the help of TEM to determine the size and shape of. Figure 7A confirmed the TEM images of AgNPs. It illustrates the most of the particles were spherical in a range of 5 to 20

nm as was reported in the case of other plant extracts as well [28,33,34]. Pronounced anisotropy among the bio-reduced nanoparticles was evident from the nanotriangles and nanoprisms.

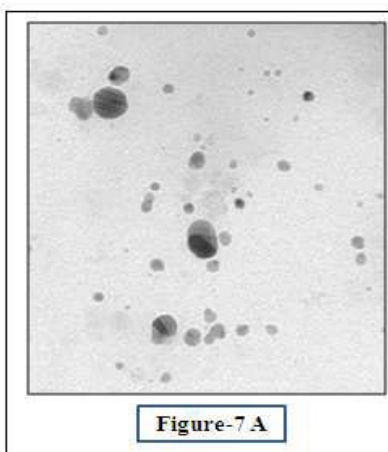


**Figure 7 (A)**  
**TEM micrographs, particle size distribution of SNP**

**DLS**

DLS measurement is  $77 \pm 1$  nm which was determined the hydrodynamic diameter of *Lycopersicon esculentum* L. AgNP, suggesting that phytochemicals (free amino acids, essential oils, variety of flavonoid glycosides) are capped on Ag nanoparticles. The stability of nanoparticle dispersion provides crucial information in change of measurement on nanoparticles and Zeta Potential ( $\zeta$ ). The long-term stability of the nanoparticulate dispersion can be used to predict the magnitude of measured zeta

potential is an indication of repulsive forces. The balances of the repulsive and attractive forces that exist among nanoparticles come within reach of the stability of nanoparticulate dispersion one another. If all the particles have a mutual repulsion, then the dispersion will remain stable [35]. However, little or no repulsion between particles, lead to aggregation. The negative zeta potential of  $-15 \pm 1$  mV for *Lycopersicon esculentum* L. - AgNP indicates that the particles repel each other and there is no tendency for the particles to aggregate (Figure 7B).

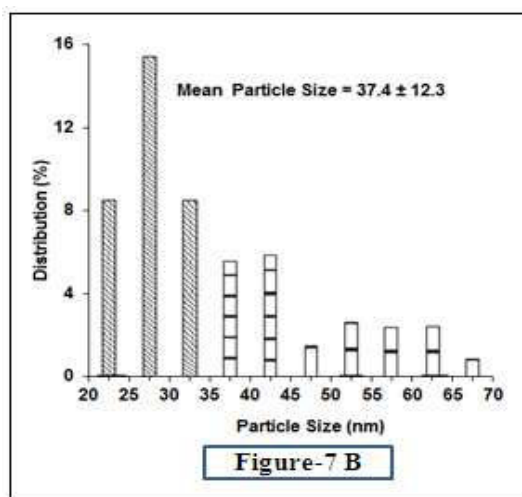


**Figure 7 (B)**  
**Corresponding SAED pattern of SNP.**

**Analysis of time kill curve demonstrates Ag nanoparticles and dose dependent killing kinetics**

The rate of possible infection of *Escherichia coli* treatments at which an antibiotic exerts its antibacterial activity is mainly significant. Therefore, the rate of AgNPs dependent killing and the time-kill assay was determined against the strain. After 6h of treatment with 200  $\mu$ M AgNPs (approximately three-fold the MBC), no colonies were recovered as shown

in Figure 8. The slopes of the kill curves analysis shown that to kill 90% of the bacterial culture could be short with the increase of AgNPs concentration along with required time; 90% of the G27 strain were killed in approximately 7h after incubation with 100  $\mu$ M AgNPs while the same amount of killing could be achieved in 3-4h upon incubation with 200  $\mu$ M AgNPs. These data's indicate dose dependent and time-dependent killing of *Escherichia coli* by AgNPs.

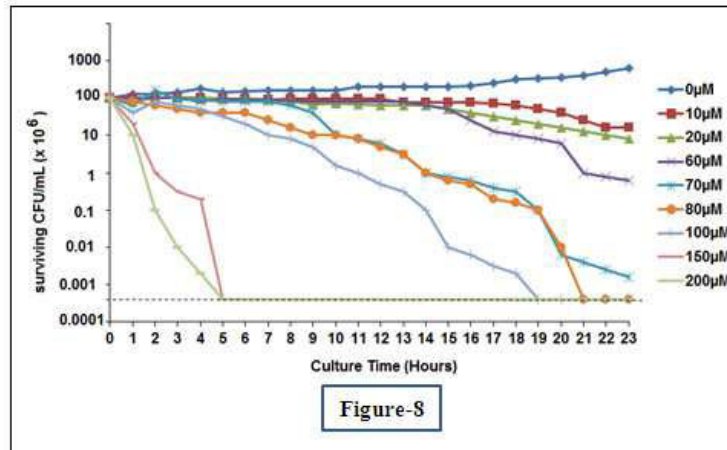


**Figure 8**

**Dose-dependent killing of *Escherichia coli* by AgNP.** Approximately  $8 \times 10^7$  cells were incubated with increasing concentrations of AgNP. The cultures were monitored for 24 h and sampled at the indicated time to determine surviving CFU by plating. The horizontal dashed line indicates the limit of detection (500 bacteria). The data are representative results from five independent experiments.

### Effect of temperature and pH on antibacterial activity of AgNPs

Antimicrobial activity of a number of drugs is widely affected by environmental circumstances like temperature and pH. The issue of temperature comes into play when one considers transport and storage of particular therapeutics, while pH stability is particularly important for *Escherichia coli* since the bacterium resides in the acidic environment of the stomach. Therefore, we tested the antimicrobial activity of AgNPs after exposure to various temperatures and acidic pH. Pre-exposure of AgNPs for 1 h to

temperatures up to  $95^{\circ}\text{C}$  did not prevent the ability of AgNPs to kill *Escherichia coli*, though there was a temperature-dependent reduction in the time required to kill all of the bacterial cells (Figure 9A). AgNPs was also active at an acidic pH (pH 4.5), but again showed delayed killing kinetics as compared to activity at a more neutral pH (pH 6.8) (Figure 9B). These data suggest that although the time to kill *Escherichia coli* is extended by high temperatures and low pH, the drug remains bactericidal against the microbe [27, 36].

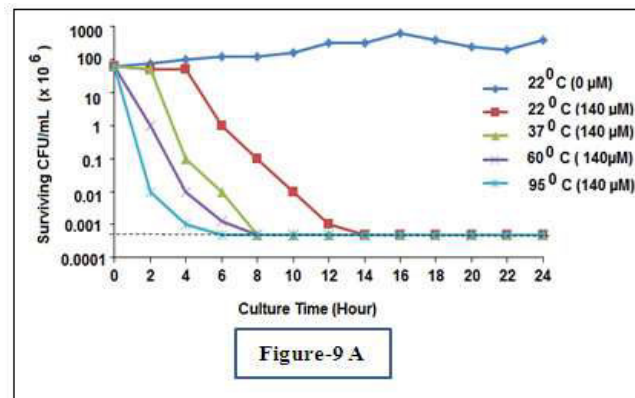


**Figure 9 A**

**Effect of temperature and low pH on the stability and bactericidal activity of AgNPs.** A) The effect of temperature on bactericidal activity of AgNPs was examined by pre-incubation of the drug at various temperatures ( $22^{\circ}\text{C}$ ,  $37^{\circ}\text{C}$ ,  $60^{\circ}\text{C}$  and  $95^{\circ}\text{C}$ ) for 1 h prior to use in the time-kill assay.

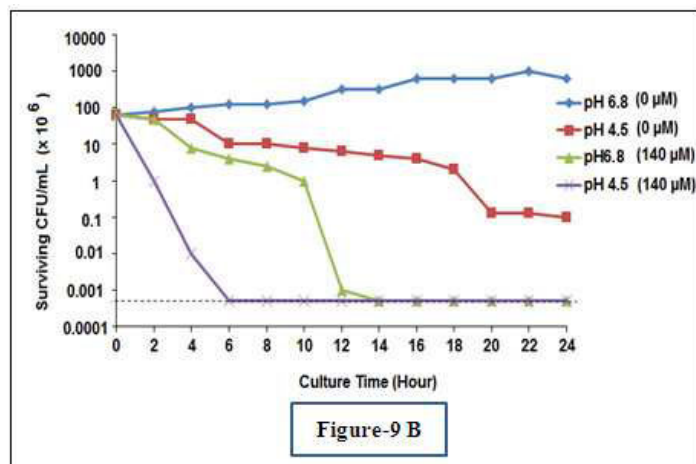


Figure 9 B

In order to determine the effect of pH on AgNPs, the time-kill assays were performed in pH-adjusted culture medium. The antibacterial activity of 140 μM AgNPs against *Escherichia coli* cultured in pH 4.5 medium was compared to bactericidal activity at pH 6.8. The plotted data are representative results from three independent experiments. The horizontal dashed line on each graph indicates the limit of detection (500 bacteria).

#### Comparison of AgNPs antibacterial activity with conventionally used anti-*Escherichia coli* antibiotics

Any newly developed anti-*Escherichia coli* drug should show better or at least comparable efficacy to antibiotics currently used in the treatment. We directly compared the antibacterial activity of AgNPs to equimolar concentrations of AMX, MTZ and CLR. Treatment with 70 μM of each of the drugs resulted in various rates of killing of the bacterial cells (Figure 10A). At this concentration, no viable *Escherichia coli* cells were recovered following 20 h of treatment with AgNPs (limit of detection = 500 bacteria). This was superior to the results

obtained with AMX and MTZ, which both showed only 2-3 logs of killing in total, but inferior to the CLR, which completely eliminated the bacterial culture after 4h of treatment (Figure 10A). Increasing the concentration of the drugs to 140 μM increased the slope of the killing curve for each of the drugs, demonstrating time and concentration dependent effects of each drug. When the bacteria were exposed to 140 μM AgNPs no detectable CFU was observed after 8h of exposure (Figure 10B). Once again, this antibacterial activity was superior to the results obtained with AMZ and MTZ, but the time for bacterial clearance was longer than for CLR (2 h) [37, 38].

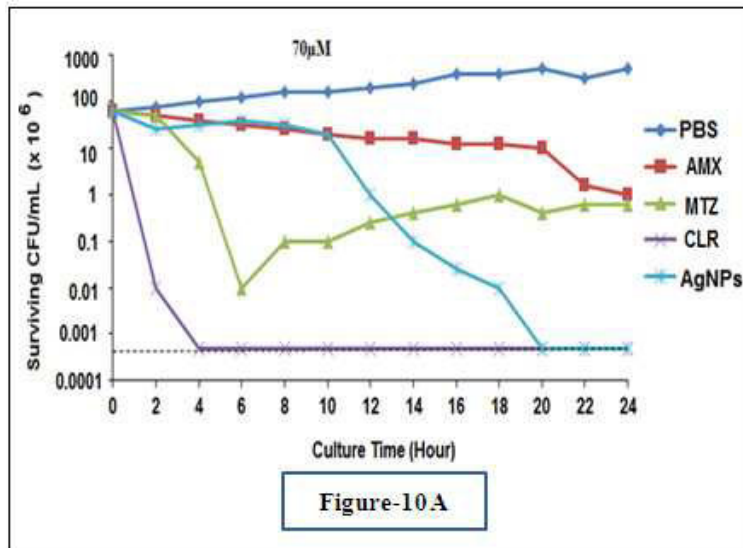


Figure-10 A

**Figure 10 A**  
*Molar-to-molar comparison of the antibacterial activity of AgNP<sub>s</sub>, amoxicillin, metronidazole, and clarithromycin. Time-kill assays for two drug concentrations, 70 μM (A) and 140 μM.*

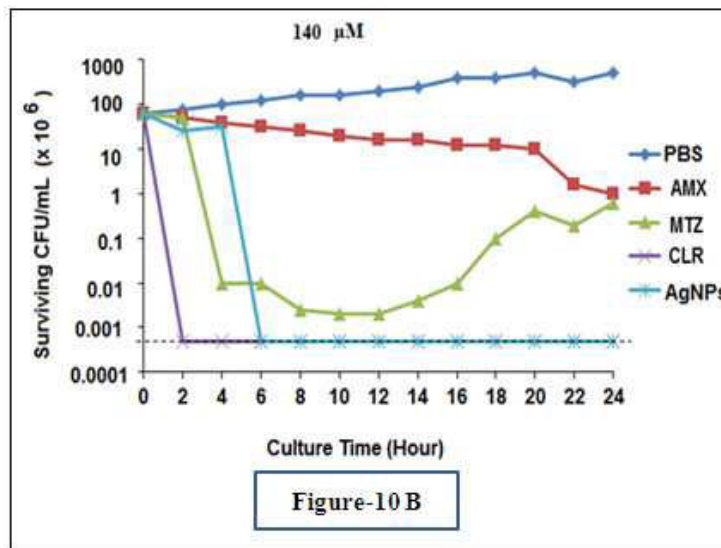


Figure-10 B

**Figure 10 B**  
*were used to compare the bactericidal activity of AgNP<sub>s</sub> to those of conventional antibiotics currently used for the treatment of H. pylori infection. The data are representative results from three independent experiments. The horizontal dashed line on each graph indicates the limit of detection (500 bacteria).*

**CONCLUSION**

The distinctive chemical, photo physical, biological and magnetic properties of silver nanoparticles may have ability to solve the need of wealthy applied and commercially viable products within the environmental, civilian, medical, defence and space exploration sectors. Therefore, intensive hard

work must be invested in the improvement of non-toxic nanoparticles for convenience in a broad spectrum of applications. Present study reported in this paper provides the role of plants to bring about a paradigms shift on future developments in nanotechnology. Our results confirm the distinctive kinetic tendency of phytochemicals which is present in *Lycopersicon esculentum* L. for reduction

of silver metal. The multipurpose phytochemical mediated green nanotechnological process has been shown to be effective in both the generation and stabilization of non-toxic Ag nanoparticles for direct applications in many of diagnostic and therapeutic applications. Ag nanoparticles will provide unprecedented opportunities towards the design and development of functional Ag nanoparticles that can be safely produced, stored and shipped worldwide.

## REFERENCES

1. Rai M, Yadav A, Plants as potential synthesizer of precious metal nanoparticles: Progress and prospects, IET Nano biotechnol. 7 (3): 117 – 24, (2013).
2. Thirunavoukkarasu M, Balaji U, Behera S, Panda PK, Mishra BK, Biosynthesis of silver nanoparticle from leaf extract of *Desmodium gangeticum* (L.) DC. And its biomedical potential, Spectrochim Acta A Mol Biomol Spectrosc., 116:424-7, (2013).
3. Mishra A, Ahmad R, Singh V, Gupta MN, Sardar M, Preparation, characterization and biocatalytic activity of a monoconjugate of alpha amylase and silver nanoparticles, J Nanosci Nanotechnol., 13(7):5028-33, (2013).
4. Arunachalam KD, Annamalai SK, *Chrysopogon zizanioides* aqueous extract mediated synthesis, characterization of crystalline silver and gold nanoparticles for biomedical applications. Int. J. Nanomedicine, 8:2375 – 84, (2013).
5. Yang BW, Guo ZY, Liu ZM, Wan MM, Qin XC, Zhong HQ, Green synthesis of silver nanoparticles and their application in SERS, Guang Pu Xue Yu Guang Pu Fen Xi (Article in Chinese), 33 (7): 1816 – 9, (2013).
6. Veerakumar K, Govindarajan M, Rajeswary M, Green synthesis of silver nanoparticles using *Sidaacuta* (Malvaceae) leaf extract against *Culex quinquefasciatus*, *Anopheles stephensi* and *Aedes aegypti* (Diptera: Culicidae). Parasitol Res., 112 (12): 4073 – 85, (2013).
7. Mochochoko T, Oluwafemi OS, Jumbam DN, Songca SP, Green synthesis of silver nanoparticles using cellulose extracted from an aquatic weed; water hyacinth. Carbohydr Polym., 98 (1): 290 – 4, (2013).
8. Narayanan KB, Park HH, Sakthivel N, Extracellular synthesis of mycogenic silver nanoparticles by *Cylindrocladium floridamum* and its homogeneous catalytic degradation of 4 – nitrophenol, Spectrochim Acta A Mol Biomol Spectrosc., 116: 485 – 90, (2013).
9. Nangmenyi G, Yue Z, Mehrabi S, Mintz E, Economy J, Synthesis and characterization of silver nanoparticle impregnated fibreglass and utility in water disinfection, Nanotechnology, 20 (9): 495705, (2009).
10. Li J, Kuang D, Feng Y, Zhang F, Xu Z, Liu M, Wang D, Green synthesis of silver nanoparticles-graphene oxide nanocomposite and its application in electrochemical sensing of tryptophan. Biosens Bioelectron., 42: 198 – 206, (2013).
11. Manikprabhu D, Lingappa K, Microwave Assisted Rapid and Green Synthesis of Silver Nanoparticles Using a Pigment Product by *Streptomyces coelicolor* klmp33. Bioinorg Chem Appl. Volume 2013, Article ID 341798, 5 pages, (2013).
12. Chiou JR, Lai BH, Hsu KC, Chen DH, One-pot green synthesis of silver/iron oxide composite nanoparticles for 4-

## ACKNOWLEDGMENT

Thanks are due to the Head of the Department of Botany, Ravenshaw University and also Director, School of Biotechnology, KIIT University for providing necessary laboratory facilities for this investigation. The authors are grateful to the Department of Botany, Berhampur University, Odisha for providing bacterial strains for this work. Authors also thank the Director CIPET, Chennai and Bhubaneswar for various analytical tests and encouragement.



- nitrophenol reduction, J Hazard Mater, 248 – 249: 394 – 400, (2013).
13. Roni M, Murugan K, Panneerselvam C, Subramaniam J, Hwang JS, Evaluation of leaf aqueous extract and synthesized silver nanoparticles using *Nerium oleander* against *Anopheles stephensi* (Diptera: Culicidae). Parasitol Res., 112 (3): 981 – 90, (2013).
  14. Sharma VK, Yngard RA, Lin Y, Silver nanoparticles: Green synthesis and their antimicrobial activities. Adv Colloid Interface Sci., 145 (1 – 2): 83 – 96, (2009).
  15. Arunachalam KD, Annamalai SK, Hari S, One-step green synthesis and characterization of leaf extract-mediated biocompatible silver and gold nanoparticles from *Memecylonum bellatum*, Int. J. Nanomedicine, 8 :1307 – 15, (2013).
  16. Zaheer Z, Rafiuddin Bio-conjugated silver nanoparticles: from *Ocimum sanctum* and role of cetyltrimethyl ammonium bromide. Colloids Surf B Biointerfaces., 108:90 – 4, (2013).
  17. Singh S, Saikia JP, Buragohain AK, A novel 'green' synthesis of colloidal silver nanoparticles (SNP) using *Dillenia indica* fruit extract, Colloids Surf Biointerfaces., 102:83 – 5, (2013).
  18. Vijayaraghavan K, Nalini SP, Prakash NU, Madhankumar D, One step green synthesis of silver nano/micro particles using extracts of *Trachyspermum ammi* and *Papaver somniferum*, Colloids Surf B Biointerfaces., 94: 114 – 7, (2012).
  19. Vidhu VK, Aromal SA, Philip D, Green synthesis of silver nanoparticles using *Macrotyloma uniflorum*, Spectrochim Acta A Mol Biomol Spectrosc., 83 (1) : 392 – 7, (2011).
  20. Haldar KM, Haldar B, Chandra G, Fabrication, characterization and mosquito larvicidal bioassay of silver nanoparticles synthesized from aqueous fruit extract of *Putranjiva*, *Drypetes roxburghii* (Wall.), Parasitol Res., 112 (4): 1452 – 9, (2013).
  21. Trebolazabala J, Maguregui M, Morillas H, de Diego A, Madariaga JM, Use of portable devices and confocal Raman Spectrometers at different wavelength to obtain the spectral information of the main organic components in tomato (*Solanum lycopersicum*) fruits, Spectrochim Acta A Mol Biomol Spectrosc., 105;391 – 9, (2013).
  22. Assor C, Quemener B, Vigouroux J, Lahaye M, Fractionation and structural characterization of LiCl – DMSO soluble hemicelluloses from tomato. Carbohydr Polym., 94 (1): 46 – 55. (2013).
  23. Park Y, Noh HJ, Han L, Kim HS, Kim YJ, Choi JS, Kim CK, Kim YS, Cho S, *Artemisia capillaris* extracts as a green factory for the synthesis of silver nanoparticles with antibacterial activities, J Nanoscience Nanotechnology., 12(9):7087 – 95, (2012).
  24. Fayaz AM, Balaji K, Girilal M, Yadav R, Kalaichelvan PT, Venketesan R, Biogenic synthesis of silver nanoparticles and their synergistic effect with antibiotics: a study against gram-positive and gram-negative bacteria, Nanomedicine, 6(1):103-9, (2010).
  25. Sharma VK, Yngard RA, Lin Y, Dilver nanoparticles: Green synthesis and their antimicrobial activities, Adv Colloid Interface Sci., 145 (1-2): 83 – 96, (2009).
  26. Kora AJ, Rastogi L, Enhancement of antibacterial activity of capped silver nanoparticles in combination with antibiotics, on model gram-negative and gram-positive bacteria. Bioinorg Chem Appl., 2013:871097, (2013).
  27. Gopinath V, MubarakAli D, Priyadarshini S, Priyadharsshini NM, Thajuddin N, Velusamy P, Biosynthesis of silver nanoparticles from *Tribulus terrestris* and its antimicrobial activity: a novel biological approach, Colloids Surf B Biointerfaces., 96:69-74, (2012).
  28. Vidhu VK, Aromal SA, Philip D, Green synthesis of silver nanoparticles using *Macrotyloma uniflorum*, Spectrochim Acta A Mol Biomol Spectrosc., 83 (1):392 – 7, (2011).
  29. Haldar KM, Haldar B, Chandra G, Fabrication, characterization and mosquito larvicidal bioassay of silver nanoparticles synthesized from aqueous fruit extract of *putranjiva*, *Drypetes roxburghii* (Wall.). Parasitol Res., 112(4):1451-9, (2013).



30. Gadadhar B, Swarnali M, and Jayasree KL, Bio-fabrication of gold nanoparticles using aqueous extract of red tomato and its use as a *colorimetric sensor*, Barman et al. *Nanoscale Research Letters*, 8:181, (2013).
31. Das J, Paul Das M, Velusamy P, *Sesbania grandiflora* leaf extract mediated green synthesis of antibacterial silver nanoparticles against selected human pathogens, *Spectrochim Acta A Mol Biomol Spectrosc.*, 104:265-70, (2013).
32. Shameli K, Bin Ahmad M, Jaffar Al-Mulla EA, Ibrahim NA, Shabanzadeh P, Rustaiyan A, Abdollahi Y, Bagheri S, Abdolmohammadi S, Usman MS, Zidan M., Green biosynthesis of silver nanoparticles using *Callicarpa maingayi* stem bark extraction, *Molecules.*,17(7):8506-17, (2012).
33. Narayanan KB, Park HH, Sakthivel N, Extracellular synthesis of mycogenic silver nanoparticles by *Cylindrocladium floridanum* and its homogeneous catalytic degradation of 4 – nitrophenol, *Spectrochim Acta A Mol Biomol Spectrosc.*, 116:485 – 90, (2013).
34. Saha S, Pal A, Kundu S, Basu S, Pal T, Photochemical green synthesis of calcium alginate stabilized Ag and Au nanoparticles and their catalytic application to 4 – nitrophenol reduction, *Langmuir*, 26 (4): 2885 – 93, (2010).
35. Mishra A, Kaushik NK, Sardar M, Sahal D, Evaluation of antiplasmodial activity of green synthesized silver nanoparticles, *Colloids Surf B Biointerfaces*, 111C:713 – 718, (2013).
36. Prakash P, Gnanaprakasam P, Emmanuel R, Arokiyaraj S, Saravanan M, Green synthesis of silver nanoparticles from leaf extract of *Mimusops elengi*, Linn. for enhanced antibacterial activity against multi drug resistant clinical isolates. *Colloids Surf B Biointerfaces.*, 108:255-9,(2013).
37. Parashar UK, Kumar V, Bera T, Saxena PS, Nath G, Srivastava SK, Giri R, Srivastava A, Study of mechanism of enhanced antibacterial activity by green synthesis of silver nanoparticles,22(41):415104,(2011)..
38. Gopinath V, MubarakAli D, Priyadarshini S, Priyadharsshini NM, Thajuddin N, Velusamy P, Biosynthesis of silver nanoparticles from *Tribulus terrestris* and its antimicrobial activity: a novel biological approach, *Colloids Surf B Biointerfaces.*, 96:69 – 74, (2012).